H. Hashimoto
Associate Professor,
Department of Mechanical & Production Engineering,
Faculty of Engineering,
Tokai University,
Kanagawa, 259-12, Japan

S. Wada
Professor,
Department of Mechanical Engineering,
School of Science and Engineering,
Waseda University,
Tokyo, Japan

M. Sumitomo
Engineer,
Mitsubishi Heavy Industries Ltd.,
1-1 Akinoura, Nagasaki-shi,
Nagasaki, Japan

The Effects of Fluid Inertia Forces on the Dynamic Behavior of Short Journal Bearings in Superlaminar Flow Regime

The effects of fluid inertia on the dynamic behavior of oil film journal bearings are theoretically investigated. The dynamic oil film forces considering the combined effects of turbulence and fluid inertia are analytically obtained under the short bearing assumption. Based on the linearized analysis, the whirl onset velocity for a balanced rigid rotor supported horizontally in the oil film journal bearings are determined initially in the case of the length-to-diameter ratio of $\lambda = 0.5$ for Reynolds numbers of $Re = 2750$, 4580, and 5500. Moreover, the nonlinear equations of motion for the rotor are solved by the improved Euler's method, and the relations between the transient journal motion and the pressure distribution corresponding to the above Reynolds numbers are examined. It is found that the fluid inertia significantly affects the dynamic behavior of turbulent journal bearings under certain operating conditions.

Introduction

It is widely recognized that oil whirl is encountered in high speed rotating machines supported in oil film journal bearings. This particular vibration is due essentially to the anisotropic nonlinear properties of oil film forces developed in the bearings, and the onset of whirl is largely influenced by the design of bearings. Since the early work by Newkirk and Taylor [1], numerous theoretical and experimental investigations have been devoted to the study of dynamic behavior of oil film journal bearings [2–13, for example]. Most of the previous investigations, however, treated only the laminar lubrication conditions. In recent years, with a continuous increase of sizes and speeds of rotating machines or with use of low kinematic viscosity lubricants such as water or liquid metals, some bearings have been subjected to both the effects of turbulence and fluid inertia. Therefore, it is of cardinal importance that these effects are taken into account in the analysis of dynamic behavior of such bearings. Although Black and Walton [14], Szeri [15], and Hashimoto and Wada [16, 17] considered the combined effects of turbulence and fluid inertia in the calculation of dynamic characteristics of the bearings, they have treated the problems based on the linearized theory. In a real situation, however, it is possible for the journal to move with considerable velocity and to reach large displacements in which a linearized treatment is not applicable. In the previous paper [18], the authors have presented an analysis concerning the dynamic characteristic problems of turbulent journal bearings based on the nonlinearized theory. But, in the analysis, the effects of fluid inertia were not considered.

The objective of this research work is to examine the effects of fluid inertia on the dynamic behavior of oil film journal bearings in superlaminar flow regime. The dynamic oil film forces considering the effects of both turbulence and fluid inertia are obtained analytically under the short bearing assumption. The nonlinear equations of motion for a balanced rigid rotor supported horizontally in the two identical aligned bearings are solved by the improved Euler's method. The journal center trajectories are calculated under three different operating conditions and the relations between the trajectories and the pressure distributions are discussed.

Theory

In the oil film journal bearings used in the high speed rotating machines such as turbines or generators, relatively small length-to-diameter ratios less than unity are employed in order to avoid an increase of power losses due to viscous friction. Therefore, in the analysis of journal motion, it may be possible to treat such bearings as the "short" journal bearings. In this paper, we firstly derive the analytical expressions for the dynamic oil film forces under the short bearing assumption.

As has been done in the previous papers [14–17], by using the averaging method, the momentum equation governing the turbulent lubrication flows in the short journal bearings as shown in Fig. 1 is expressed as:

Contributed by the Tribology Division of The American Society of Mechanical Engineers and presented at the ASLE/ASME Tribology Conference, San Antonio, Texas, October 5–8, 1987. Manuscript received by the Tribology Division February 3, 1987. Paper No. 87-Trib-43.

Copyright © 1988 by ASME

Downloaded 16 Aug 2012 to 165.91.101.108. Redistribution subject to ASME license or copyright; see http://www.asme.org/terms/Terms_Use.cfm

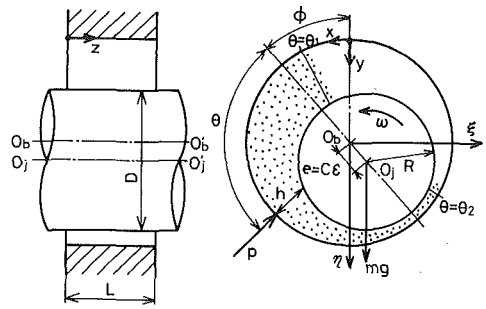

Fig. 1 Geometry of short journal bearing

$$\rho\left(\frac{\partial q_z}{\partial t}+\frac{R\omega}{2}\frac{\partial q_z}{\partial x}+\frac{1}{h}\frac{\partial q_z^2}{\partial z}\right)=-h\frac{\partial p}{\partial z}-\frac{\mu q_z}{h^2G_z} \quad (1)$$

The averaged form of the equation of continuity is:

$$\frac{R\omega}{2}\frac{\partial h}{\partial x}+\frac{\partial q_z}{\partial z}+\frac{\partial h}{\partial t}=0 \quad (2)$$

where q_z indicates the axial flow rate, which is defined by:

$$q_z=\int_0^h w dy \quad (3)$$

The film thickness h and the turbulence coefficient G_z are given respectively as follows [18]:

$$h=C(1+\epsilon\cos\theta) \quad (4)$$

$$G_z=\frac{1}{12(a_z+b_z\epsilon\cos\theta)} \quad (5)$$

where:

$$a_z=1+0.00069\mathrm{Re}^{0.88},\ b_z=0.00061\mathrm{Re}^{0.88} \quad (6)$$

In the analysis, the following nondimensional quantities are introduced.

$$\bar{h}=\frac{h}{C},\ \bar{p}=\frac{pC^2}{\mu R^2\omega},\ \epsilon=\frac{e}{C},$$

$$\bar{q}_z=\frac{q_z}{CR\omega},\ \mathrm{Re}=\frac{\rho CR\omega}{\mu},$$

$$\mathrm{Re}^*=\frac{\rho C^2\omega}{\mu},\ \lambda=\frac{L}{D},\ \bar{t}=\omega t,\ \bar{z}=\frac{z}{L},\ \theta=\frac{x}{R}-\phi \quad (7)$$

Substituting these quantities into equations (1) and (2), these equations are normalized as follows:

$$\mathrm{Re}^*\left(\frac{\partial\bar{q}_z}{\partial\bar{t}}+\frac{1}{2}\frac{\partial\bar{q}_z}{\partial\theta}+\frac{1}{2\lambda\bar{h}}\frac{\partial\bar{q}_z^2}{\partial\bar{z}}\right)=-\frac{1}{2\lambda}\bar{h}\frac{\partial\bar{p}}{\partial\bar{z}}-\frac{\bar{q}_z}{\bar{h}^2G_z} \quad (8)$$

$$\frac{1}{2}\frac{\partial\bar{h}}{\partial\theta}+\frac{1}{2\lambda}\frac{\partial\bar{q}_z}{\partial\bar{z}}+\frac{\partial\bar{h}}{\partial\bar{t}}=0 \quad (9)$$

Integrating equation (9) with respect to $\bar{z}$, with the condition $\bar{q}_z=0$ at $\bar{z}=0.5$, the axial flow rate $\bar{q}_z$ is obtained as:

$$\bar{q}_z=-2\lambda\left(\frac{1}{2}\frac{\partial\bar{h}}{\partial\theta}+\frac{\partial\bar{h}}{\partial\bar{t}}\right)\left(\bar{z}-\frac{1}{2}\right) \quad (10)$$

Substitution of equation (10) into equation (8) yields the following pressure gradient equation.

$$\frac{\partial\bar{p}}{\partial\bar{z}}=\left[\frac{4\lambda^2\mathrm{Re}^*}{\bar{h}}\left\{\frac{\partial^2\bar{h}}{\partial\bar{t}^2}+\frac{\partial^2\bar{h}}{\partial\theta\partial\bar{t}}+\frac{1}{4}\frac{\partial^2\bar{h}}{\partial\theta^2}-\frac{2}{\bar{h}}\left(\frac{1}{2}\frac{\partial\bar{h}}{\partial\theta}+\frac{\partial\bar{h}}{\partial\bar{t}}\right)^2\right\}+\frac{4\lambda^2}{\bar{h}^3G_z}\left(\frac{1}{2}\frac{\partial\bar{h}}{\partial\theta}+\frac{\partial\bar{h}}{\partial\bar{t}}\right)\right]\left(\bar{z}-\frac{1}{2}\right) \quad (11)$$

Integrating equation (11) with respect to $\bar{z}$, with the condition $\bar{p}=0$ at $\bar{z}=1$, and substituting equations (4) and (5), the dimensionless dynamic oil film pressure is obtained as:

$$\bar{p}=-\frac{\lambda^2\mathrm{Re}^*}{2(1+\epsilon\cos\theta)}\left[4(\ddot{\epsilon}\cos\theta+\epsilon\ddot{\phi}\sin\theta)-(1-2\dot{\phi})\{(1-2\dot{\phi})\epsilon\cos\theta+4\dot{\epsilon}\sin\theta\}-\frac{2\{(1-2\dot{\phi})\epsilon\sin\theta-2\dot{\epsilon}\cos\theta\}^2}{1+\epsilon\cos\theta}\right]\bar{z}(1-\bar{z})$$

Nomenclature

a_z, b_z = coefficients defined in equation (6)
$b_{ij}(i,j=\xi,\eta)$ = damping coefficients
$\bar{b}_{ij}(i,j=\xi,\eta)$ = $C^3b_{ij}/(\mu R^3L)$ = dimensionless damping coefficients
C = radial clearance
$c_{ij}(i,j=\xi,\eta)$ = acceleration coefficients
$\bar{c}_{ij}(i,j=\xi,\eta)$ = $C^3c_{ij}\omega/(\mu R^3L)$ = dimensionless acceleration coefficients
D = journal diameter
e = eccentricity of the journal center
f_1-f_9 = functions defined in equation (19)
F_ϵ = oil film froce component along the line of centers
F_ϕ = oil film force component normal to the line of centers
$\bar{F}_\epsilon$ = $C^2F_\epsilon/(\mu R^3L\omega)$ = dimensionless oil film force component along the line of centers
$\bar{F}_\phi$ = $C^2F_\phi/(\mu R^3L\omega)$ = dimensionless oil film force component normal to the line of centers
g = gravitational acceleration
G_z = turbulence coefficient
h = oil film thickness
$\bar{h}$ = h/C = dimensionless oil film thickness
I_1-I_7 = functions defined in equation (17)
J_1-J_7 = functions defined in equation (18)
$k_{ij}(i,j=\xi,\eta)$ = spring coefficients
$\bar{k}_{ij}(i,j=\xi,\eta)$ = $C^3k_{ij}/(\mu R^3L\omega)$ = dimensionless spring coefficients
L = bearing length
m = reduced mass of rotor per bearing
n = rotating shaft speed per unit time
p = oil film pressure
$\bar{p}$ = $pC^2/(\mu R^2\omega)$ = dimensionless oil film pressure
q_z = oil flow rate in the axial direction
$\bar{q}_z$ = $q_z/(CR\omega)$ dimensionless oil flow rate in the axial direction
R = journal radius
Re = $\rho CR\omega/\mu$ = mean Reynolds number
Re* = $\rho C^2\omega/\mu$ = inertia parameter

Downloaded 16 Aug 2012 to 165.91.101.108. Redistribution subject to ASME license or copyright; see http://www.asme.org/terms/Terms_Use.cfm

$$+\frac{12\lambda^2(a_z+b_z\epsilon\cos\theta)\{(1-2\dot{\phi})\epsilon\sin\theta-2\dot{\epsilon}\cos\theta\}}{(1+\epsilon\cos\theta)^3}\bar{z}(1-\bar{z}) \quad (12)$$

Assuming the oil film rupture in the negative pressure region, the dimensionless oil film force components along and normal to the line of centers, $\bar{F}_\epsilon$ and $\bar{F}_\phi$, are given respectively by integrating the oil film pressure over the positive pressure region ($\theta_1 \leqq \theta \leqq \theta_2$) as:

$$\bar{F}_\epsilon = -\int_0^1\int_{\theta_1}^{\theta_2} \bar{p}\cos\theta d\theta d\bar{z} \quad (13)$$

$$\bar{F}_\phi = \int_0^1\int_{\theta_1}^{\theta_2} \bar{p}\sin\theta d\theta d\bar{z} \quad (14)$$

By using the prescribed values of displacements, velocities and accelerations of the journal center, the angles θ_1 and θ_2 are estimated numerically by solving the nonlinear equations with respect to θ, which is obtained by putting $p=0$ in equation (12).

Substituting equation (12) into equations (13) and (14) and carrying out the integration by making use of the Sommerfeld substitution, we have:

$$\bar{F}_\epsilon = -\frac{\lambda^2\mathrm{Re}^*}{3}\Big\{\ddot{\epsilon}I_1+\ddot{\phi}I_2+\dot{\epsilon}^2I_3+\dot{\epsilon}(1-2\dot{\phi})I_4 + (1-2\dot{\phi})^2I_5\Big\}+2\lambda^2\{(1-2\dot{\phi})I_6+\dot{\epsilon}I_7\} \quad (15)$$

$$\bar{F}_\phi = -\frac{\lambda^2\mathrm{Re}^*}{3}\Big\{\ddot{\epsilon}J_1+\ddot{\phi}J_2+\dot{\epsilon}^2J_3+\dot{\epsilon}(1-2\dot{\phi})J_4+(1-2\dot{\phi})^2J_5\Big\} + 2\lambda^2\{(1-2\dot{\phi})J_6+\dot{\epsilon}J_7\} \quad (16)$$

where:

$$I_1 = \frac{1}{\epsilon^2}\left(f_1-\epsilon f_2-\frac{1}{\sqrt{1-\epsilon^2}}f_8\right),\ I_2 = \frac{1}{\epsilon}\left(\epsilon f_3-f_9\right),$$

$$I_3 = \frac{2}{\epsilon^3}\left\{-2f_1+\frac{2-3\epsilon^2}{(1-\epsilon^2)^{3/2}}f_8+\frac{\epsilon}{1-\epsilon^2}f_5+\epsilon f_2\right\},$$

$$I_4 = \frac{1}{\epsilon^2}\left(\epsilon f_3-2f_4-3f_9\right),$$

$$I_5 = \frac{1}{4\epsilon}\left(3f_1-\epsilon f_2-\frac{3-2\epsilon^2}{\sqrt{1-\epsilon^2}}f_8-2\epsilon f_5\right),$$

$$I_6 = \frac{1}{2\epsilon}\left\{2b_zf_9-2(a_z-2b_z)f_4+(a_z-b_z)f_6\right\},$$

$$I_7 = \frac{1}{\epsilon^2}\left[2b_zf_1-\frac{2\epsilon\{b_z+(2a_z-3b_z)\epsilon^2\}}{(1-\epsilon^2)^2}f_5 + \frac{(a_z-b_z)\epsilon^2}{(1-\epsilon^2)^2}f_7 + \frac{2(a_z-3b_z)\epsilon^4+(a_z+5b_z)\epsilon^2-2b_z}{(1-\epsilon^2)^{5/2}}f_8\right], \quad (17)$$

$$J_1 = \frac{1}{\epsilon^2}\left(-\epsilon f_3+f_9\right),\ J_2 = \frac{1}{\epsilon}\left(f_1-\epsilon f_2-\sqrt{1-\epsilon^2}f_8\right),$$

$$J_3 = \frac{2}{\epsilon^3}\left(\epsilon f_3-f_4-2f_9\right),$$

$$J_4 = \frac{1}{\epsilon^2}\left(3f_1-\epsilon f_2-2\epsilon f_5-\frac{3-\epsilon^2}{\sqrt{1-\epsilon^2}}f_8\right),$$

$$J_5 = \frac{1}{4\epsilon}\left\{-\epsilon f_3+2(1-\epsilon^2)f_4+3f_9\right\},$$

$$J_6 = \frac{1}{2\epsilon}\left\{-2b_zf_1+2b_z\epsilon f_5-\frac{(a_z-b_z)\epsilon^2}{1-\epsilon^2}f_7 + \frac{(a_z-3b_z)\epsilon^2+2b_z}{(1-\epsilon^2)^{3/2}}f_8\right\},$$

$$J_7 = \frac{1}{\epsilon^2}\left\{-2(a_z-2b_z)f_4+(a_z-b_z)f_6+2b_zf_9\right\} \quad (18)$$

where the functions f_i ($i=1-9$) are given as:

Nomenclature (cont.)

S = $2\mu nLR^3/(mgC^2)$ = Sommerfeld number
t = time
$\bar{t}$ = ωt = dimensionless time
w = velocity component in the axial direction
x = coordinate in the rotating direction, Fig. 1
y = coordinate in the film thickness direction, Fig. 1
z = coordinate in the axial direction, Fig. 1
$\bar{z}$ = z/L = dimensionless coordinate in the axial direction
α, β = dimensionless coefficients defined in equation (23)
ϵ = e/C = eccentricity ratio
η = coordinate in the vertical direction, Fig. 1
$\bar{\eta}$ = η/C = dimensionless coordinate in the vertical direction, Fig. 1
θ = $x/R-\phi$ = circumferential coordinate, Fig. 1
λ = L/D = length-to-diameter ratio
μ = viscosity
ξ = coordinate in the horizontal direction, Fig. 1
$\bar{\xi}$ = ξ/C = dimensionless coordinate in the horizontal direction
ρ = density
ϕ = attitude angle
ω = angular velocity of rotating shaft
ω_{cr} = whirl onset velocity
$\bar{\omega}_{cr}$ = $\omega_{cr}\sqrt{C/g}$ = dimensionless whirl onset velocity

Subscripts

ϵ = direction along the line of centers
η = vertical direction
ξ = horizontal direction
ϕ = direction normal to the line of centers
1 = starting position of positive pressure region
2 = final position of positive pressure region

Superscript

= dimensionless time derivative

Downloaded 16 Aug 2012 to 165.91.101.108. Redistribution subject to ASME license or copyright; see http://www.asme.org/terms/Terms_Use.cfm

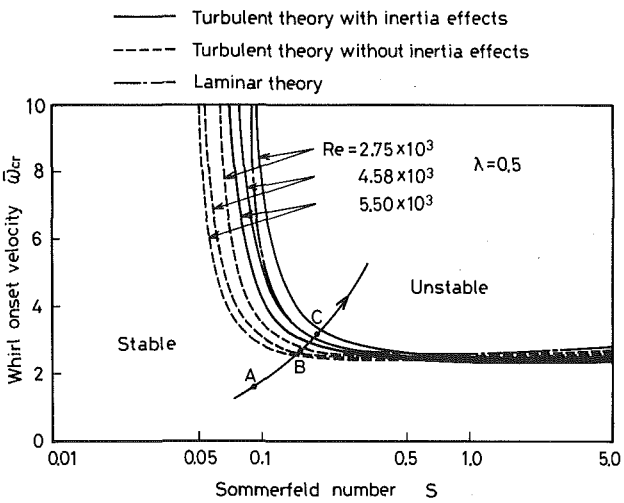

Fig. 2 Variation in whirl onset velocity with Sommerfeld number

$$f_1 = \theta_2 - \theta_1, f_2 = \sin\theta_2 - \sin\theta_1, f_3 = \cos\theta_2 - \cos\theta_1,$$

$$f_4 = \frac{1}{1+\epsilon\cos\theta_2} - \frac{1}{1+\epsilon\cos\theta_1},$$

$$f_5 = \frac{\sin\theta_2}{1+\epsilon\cos\theta_2} - \frac{\sin\theta_1}{1+\epsilon\cos\theta_1},$$

$$f_6 = \frac{1}{(1+\epsilon\cos\theta_2)^2} - \frac{1}{(1+\epsilon\cos\theta_1)^2},$$

$$f_7 = \frac{\sin\theta_2(\epsilon+\cos\theta_2)}{(1+\epsilon\cos\theta_2)^2} - \frac{\sin\theta_1(\epsilon+\cos\theta_2)}{(1+\epsilon\cos\theta_1)^2},$$

$$f_8 = \sin^{-1}\left(\frac{\sqrt{1-\epsilon^2}\sin\theta_2}{1+\epsilon\cos\theta_2}\right) - \sin^{-1}\left(\frac{\sqrt{1-\epsilon^2}\sin\theta_1}{1+\epsilon\cos\theta_1}\right),$$

$$f_9 = \ln\left(\frac{1+\epsilon\cos\theta_2}{1+\epsilon\cos\theta_1}\right) \tag{19}$$

When we put $\mathrm{Re}^* = 0$ in equations (15) and (16), the expressions of oil film force components for the case of inertialess turbulent flow are obtained. In addition, when we put $\mathrm{Re} = 0$, the expressions for the case of laminar flow are obtained. Linearizing equations (15) and (16) around the static equilibrium position of the journal center and converting the polar coordinates (ϵ, ϕ) to cartesian coordinates (ξ, η) as shown in Fig. 1, the fluctuating oil film force components in the horizontal and vertical directions are expressed as follows:

$$\begin{bmatrix} d\bar{F}_\xi \\ d\bar{F}_\eta \end{bmatrix} = \begin{bmatrix} \bar{k}_{\xi\xi} & \bar{k}_{\xi\eta} \\ \bar{k}_{\eta\xi} & \bar{k}_{\eta\eta} \end{bmatrix} \begin{bmatrix} \bar{\xi} \\ \bar{\eta} \end{bmatrix} + \begin{bmatrix} \bar{b}_{\xi\xi} & \bar{b}_{\xi\eta} \\ \bar{b}_{\eta\xi} & \bar{b}_{\eta\eta} \end{bmatrix} \begin{bmatrix} \dot{\bar{\xi}} \\ \dot{\bar{\eta}} \end{bmatrix} + \begin{bmatrix} \bar{C}_{\xi\xi} & \bar{C}_{\xi\eta} \\ \bar{C}_{\eta\xi} & \bar{C}_{\eta\eta} \end{bmatrix} \begin{bmatrix} \ddot{\bar{\xi}} \\ \ddot{\bar{\eta}} \end{bmatrix} \tag{20}$$

Substituting equation (20) into the equations of motion for a balanced rigid rotor supported horizontally in the identical two aligned bearings and applying the Routh-Hurwitz stability criterion to the equations, the whirl onset velocity $\bar{\omega}_{cr}$, including the combined effects of turbulence and fluid inertia, is determined. However, such a linearized stability analysis predicts only the stability limits of rotor-bearing systems, and it does not give any information concerning the transient behavior of rotors below and above the stability limits. Therefore, the following nonlinear analysis is necessary to obtain such information.

From the force balance at the journal center, in the directions along and normal to the line of centers, the nonlinear equations of motion for a balanced rigid rotor supported horizontally are expressed as follows [18]:

$$m\left\{\frac{d^2e}{dt^2} - e\left(\frac{d\phi}{dt}\right)^2\right\} = -F_\epsilon + mg\cos\phi \tag{21}$$

$$m\left\{e\frac{d^2\phi}{dt^2} + 2\left(\frac{de}{dt}\right)\left(\frac{d\phi}{dt}\right)\right\} = F_\phi - mg\sin\phi \tag{22}$$

Normalizing these equations, we have:

$$\ddot{\epsilon} - \epsilon\dot{\phi}^2 = -\alpha\bar{F}_\epsilon + \beta\cos\phi \tag{23}$$

$$\epsilon\ddot{\phi} + 2\dot{\epsilon}\dot{\phi} = \alpha\bar{F}_\phi + \beta\sin\phi \tag{24}$$

where:

$$\alpha = \frac{\mu R^3 L}{mC\omega^3}, \quad \beta = \frac{g}{C\omega^2} \tag{25}$$

The improved Euler's method is applied to integrate a set of dimensionless nonlinear equations (23) and (24) forward in time, in which the oil film force components $\bar{F}_\epsilon$ and $\bar{F}_\phi$ are given analytically by equations (15) and (16). The starting and final positions of positive pressure region θ_1 and θ_2, which are included in equations (15) and (16), are calculated by using the displacements, velocities and accelerations of the journal center previously obtained at the prior time step.

Results and Discussion

Sample numerical results were obtained under the following data.

The diameter and length of journal bearing, D and L, are 0.07 m and 0.035 m, respectively. Then, the length-to-diameter ratio, λ, takes value of 0.5. The load on the journal, mg, is 26.5 N per bearing. The viscosity and density of lubricants, μ and ρ, are 1.0×10^{-3} Pa.s and 1.0×10^3 kg/m^3, respectively, and the radial clearance of bearing C is 2.5×10^{-4} m. The calculations are made for three different rotating shaft speeds of $n = 50$ rps, 83.3 rps and 100 rps. The Reynolds numbers for each speed are $\mathrm{Re} = 2750$, 4580 and 5500, and the corresponding inertia parameters are $\mathrm{Re}^* = 19.6$, 32.7, and 39.3.

The whirl onset velocities calculated from three types of lubrication theories are illustrated in Fig. 2, in which the lower and upper sides of each curve are corresponding to stable and unstable regions, respectively. The solid lines indicate the results obtained from the turbulent theory with inertia effects, the dashed lines the results from the theory without inertia effects and the dot-dashed line the results from the conventional laminar theory. The points A, B, and C are corresponding to the cases of rotating shaft speeds of $n = 50$ rps, 83.3 rps and 100 rps, respectively. The results from the laminar theory show that the behavior of journal motion finally becomes stable at the points A and B and unstable at the point C. When the turbulent effects are considered, the results show the different situations. In such a case, the journal is stable at the point A and unstable at the points B and C. However, when the inertia effects are considered in addition to the turbulent effects, the results show again that the journal becomes stable at the points A and B and unstable at the point C just as predicted from the laminar theory. Then, it is concluded that the inertia effects contribute to enhancing the stability of rotor-bearing systems under certain operating conditions.

The relations between the transient journal motion and the pressure distribution are examined for the different operating conditions indicated by the three points in Fig. 2. The journal center trajectory is started at the position near by the concentric point between journal and bearing, and the initial values of velocities and accelerations of the journal center are set

Downloaded 16 Aug 2012 to 165.91.101.108. Redistribution subject to ASME license or copyright; see http://www.asme.org/terms/Terms_Use.cfm

equal to zero. The time increment used in the calculation, $\Delta\bar{t}$, is 0.063.

Figures 3 to 5 show the results obtained from three types of lubrication theories for a balanced rigid rotor. The results at point A are demonstrated in Figs. 3(*a*) to 3(*c*). In all theories, the path of journal center rapidly approaches to the static equilibrium position and the journal becomes stable as predicted in Fig. 2. As can be seen from the variation of pressure distribution, the wedge film action is always dominant and squeeze film effects are negligibly small during the journal motion, so the oil film pressure is well behaved throughout the trajectory. The turbulence has insignificant influence on the transient pressure, but the fluid inertia considerably enlarges the positive pressure region. As a result, the journal moves upward due to inertia effects.

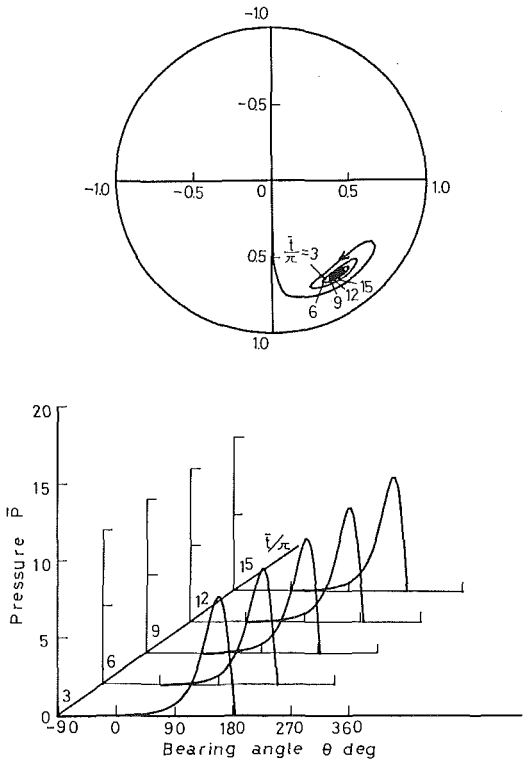

Fig. 3(*a*) Journal center trajectory and pressure distribution at point A (laminar theory, $n = 50$ rps)

Figures 4(*a*) to 4(*c*) show the results at point B. The path of journal center calculated from the laminar theory gradually approaches to the static equilibrium position and the journal finally becomes stable as shown in Fig. 4(*a*). In such a case, the wedge film action is dominant in the oil film and then the pressure distribution is varying little with the passage of time. When the turbulent effects are considered, different behavior of journal motion is observed. In Fig. 4(*b*), the path of journal center calculated from the turbulent theory without inertia effects show the growing spiral form, and if more cycle were run the trajectory would reach a large limit cycle and the journal would continue the violent whirling in a circular orbital path. When the journal reaches the clearance circle, the "positive" squeeze film action is dominant and a large positive pressure peak occurs near the position of film rupture, while when the journal reaches the bearing center, the "negative" squeeze action is dominant and then the pressure becomes small. Such a variation in pressure distribution with the passage of time results in an instability of the rotor-bearing systems. On the other hand, the path of journal center calculated from the turbulent theory with inertia effects gradually approaches the static equilibrium position and the journal becomes stable as shown in Fig. 4(*c*). In this case, the wedge film action is dominant in the oil film and the pressure distribution is varying little as time progresses. Since the positive pressure region is enlarged with inertia effects, the static equilibrium position moves upward compared with the position obtained from the laminar theory. It can be seen from this figure that the inertia

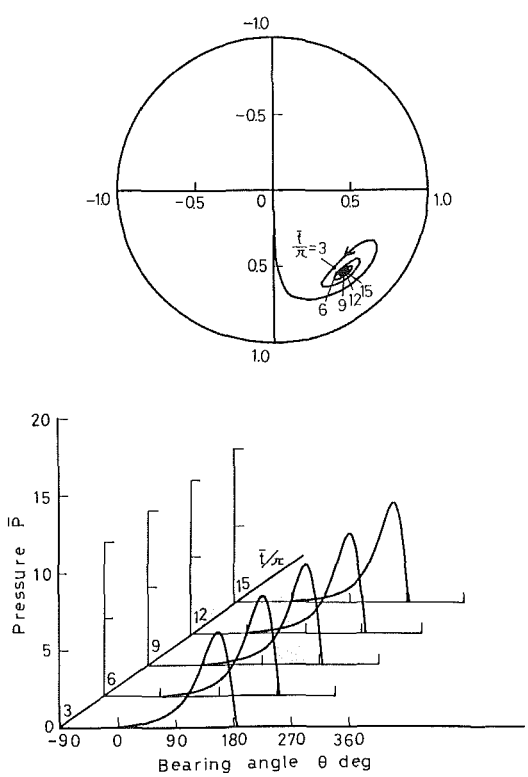

Fig. 3(*b*) Journal center trajectory and pressure distribution at point A (turbulent theory without inertia effects, $n = 50$ rps)

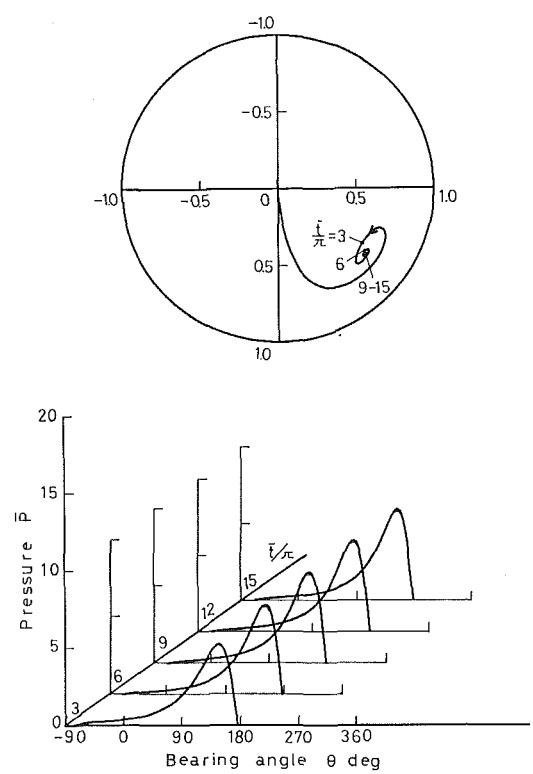

Fig. 3(*c*) Journal center trajectory and pressure distribution at point A (turbulent theory with inertia effects, $n = 50$ rps)

Downloaded 16 Aug 2012 to 165.91.101.108. Redistribution subject to ASME license or copyright; see http://www.asme.org/terms/Terms_Use.cfm

forces have an ability of enhancing the stability, and it may be necessary to take into account the effects in order to adequately analyze the dynamic behavior of the bearings.

The results at the point C are indicated in Figs. 5(*a*) to 5(*c*). In this case, the path of journal center takes a growing spiral form and it reaches finally a large limit cycle for all theories.

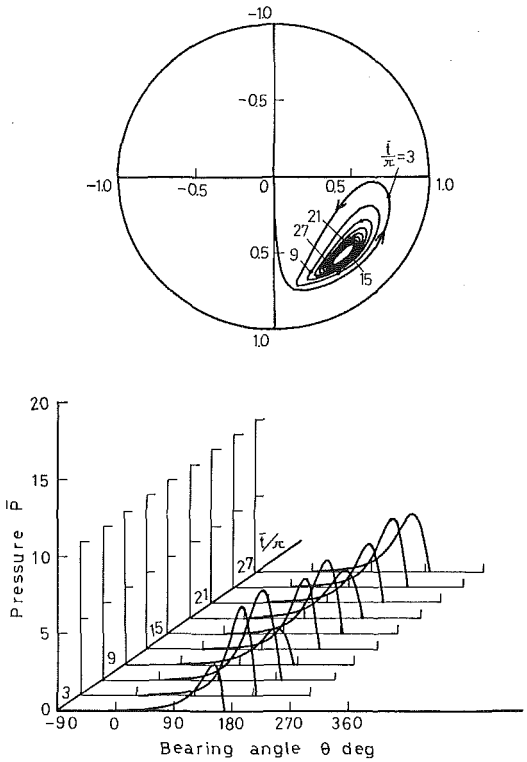

Fig. 4(*a*) Journal center trajectory and pressure distribution at point B (laminar theory, $n = 83.3$ rps)

The journal continues the violent whirling with whirl ratio of approximately 0.5. When the journal reaches the clearance circle, a large positive pressure peak occurs near the position of film rupture. On the other hand, when the journal reaches the bearing center, the pressure becomes very small. As a result of such violent variation of pressure distribution, the journal becomes unstable. Comparing Figs. 5(*b*) and 5(*c*), it is found that the inertia effects lose an advantage of enhancing the stability under such operating condition.

Conclusions

The authors have investigated theoretically the effects of fluid inertia on the dynamic behavior of oil film journal bearings in superlaminar flow regime. The dynamic oil film forces considering the effects of both turbulence and fluid inertia were obtained under the short bearing assumption. The nonlinear equations of motion for a balanced rigid rotor supported horizontally in the identical two aligned bearings were solved by the improved Euler's method, and the relations between the transient journal motion and the pressure distribution were examined under three different operating conditions. Sample numerical results obtained were demonstrated in graphical form for the length-to-diameter ratio of $\lambda = 0.5$. The effects of fluid inertia on the dynamic behavior of oil film journal bearings are even more pronounced than those of turbulence, and the inertia effects contribute to enhancing the stability of rotor-bearing systems under certain operating conditions. Therefore, it may be necessary to take into account the inertia effects in order to adequately analyze the dynamic behavior of turbulent journal bearings.

References

1 Newkirk, B. L., and Taylor, H. D., "Shaft Whipping Due to Oil Action in Journal Bearings," *Gen. Electr. Rev.*, Vol. 28, 1925, pp. 985–988.

2 Hori, Y., "A Theory of Oil Whip," ASME *Journal of Applied Mechanics*, Vol. 81, 1959, pp. 189–198.

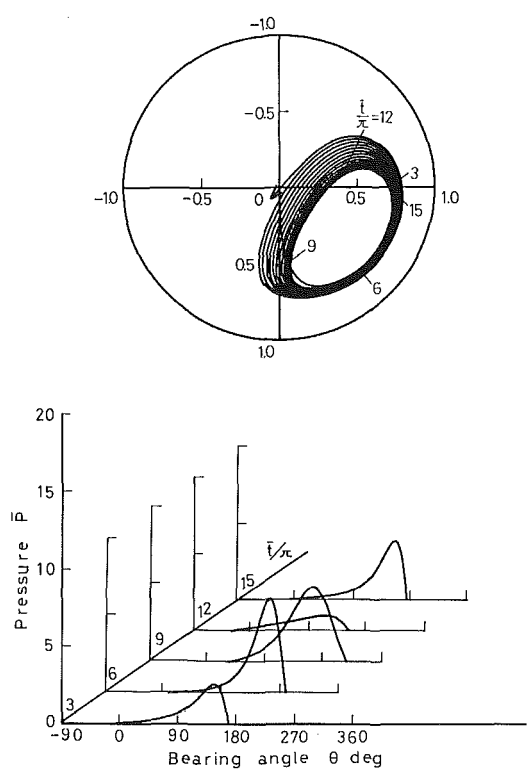

Fig. 4(*b*) Journal center trajectory and pressure distribution at point B (turbulent theory without inertia effects, $n = 83.3$ rps)

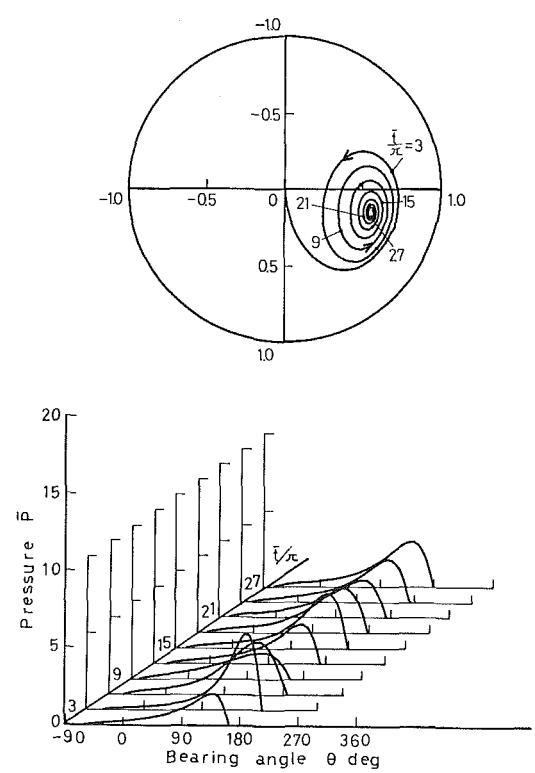

Fig. 4(*c*) Journal center trajectory and pressure distribution at point B (turbulent theory with inertia effects, $n = 83.3$ rps)

Downloaded 16 Aug 2012 to 165.91.101.108. Redistribution subject to ASME license or copyright; see http://www.asme.org/terms/Terms_Use.cfm

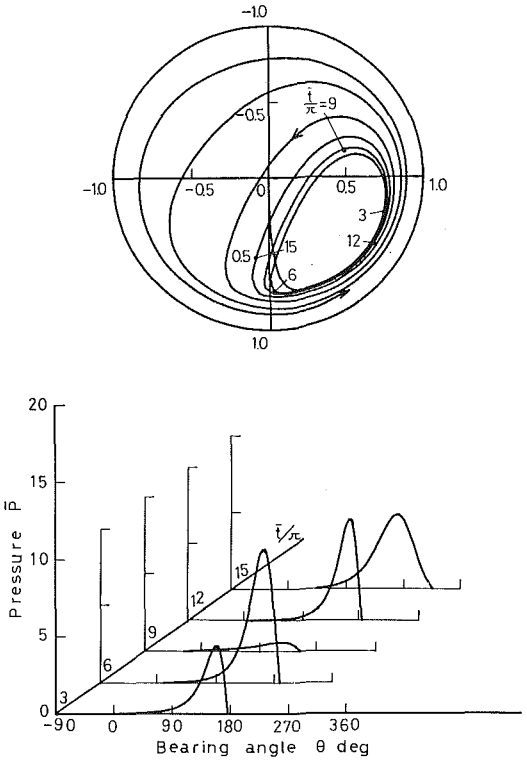

Fig. 5(*a*) Journal center trajectory and pressure distribution at point C (laminar theory, $n = 100$ rps)

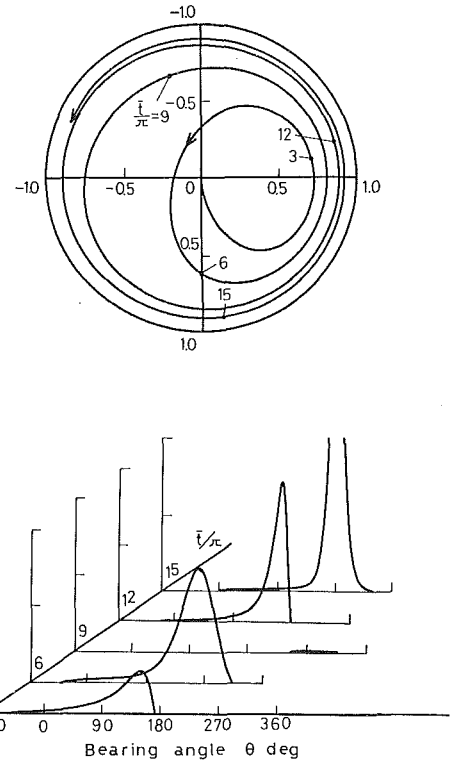

Fig. 5(*c*) Journal center trajectory and pressure distribution at point C (turbulent theory with inertia effects, $n = 100$ rps)

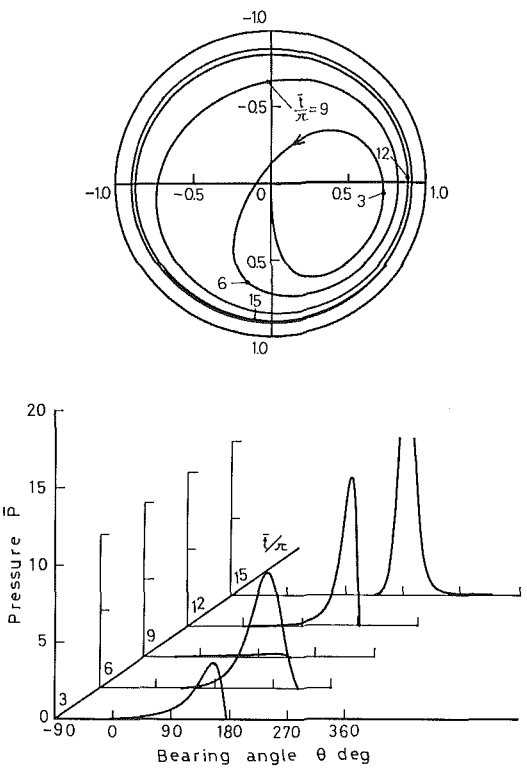

Fig. 5(*b*) Journal center trajectory and pressure distribution at point C (turbulent theory without inertia effects, $n = 100$ rps)

3 Holmes, R., "The Vibration of a Rigid Shaft on Short Sleeve Bearings," *J. Mech. Eng. Sci.*, Vol. 2, No. 4, 1960, pp. 337–341.

4 Reddi, M. M., and Trumpler, P. R., "Stability of the High-Speed Journal Bearings Under Steady Load," ASME *Journal of Engineering for Industry*, Vol. 84, 1962, pp. 351–358.

5 Lund, J. W., and Saibel, E., "Oil Whip Orbits of a Rotor in Sleeve Bearings," ASME *Journal of Engineering for Industry*, Vol. 89, 1967, pp. 813–823.

6 Badgley, H., and Booker, J. F., "Turborotor Instability-Effect of Initial Transients on Plane Motion," ASME Journal of Lubrication Technology, Vol. 91, 1969, pp. 625–633.

7 Akers, A., Michaelson, S., and Cameron, A., "Stability Contours for a Whirling Finite Journal Bearing," ASME Journal of Lubrication Technology, Vol. 93, 1971, p. 177–190.

8 Kirk, R. G., and Gunter, E. J., "Short Bearing Analysis Applied to Rotor Dynamics. Part 1: Theory," ASME Journal of Lubrication Technology, Vol. 98, 1976, pp. 47–56.

9 Kirk, R. G., and Gunter, E. J., "Short Bearing Analysis Applied to Rotor Dynamics. Part 2: Results of Journal Bearing Response," ASME Journal of Lubrication Technology, Vol. 98, 1976, pp. 319–329.

10 Grosby, W. A., "The Stability of a Rigid Rotor in Ruptured Finite Journal Bearings," *Wear*, Vol. 80, 1982, pp. 333–346.

11 Akkök, M., and Ettles, C. M. McC, "Journal Bearing Response to Excitation and Behavior in the Unstable Region," *ASLE Trans.*, Vol. 27, No. 4, 1984, pp. 341–351.

12 Brindley, J., Elliott, L., and Mckay, J. T., "The Role of Cavitation in Whirl Instability in a Rotor Bearing," ASME *Journal of Applied Mechanics*, Vol. 50, 1983, pp. 877–885.

13 Holmes, A. G., Ettles, C. M. M., and Mayes, I. W., "Aperiodic Behavior of a Rigid Shaft in Short Journal Bearings," *International Journal of Numerical Method in Engineering*, Vol. 12, 1978, pp. 695–702.

14 Black, H. F., and Walton, M. H., "Theoretical and Experimental Investigations of a Short 360° Journal Bearing in the Transition Superlaminar Regime," *Journal of Mechanical Engineering Science*, Vol. 16, 1974, pp. 286–297.

15 Seri, A. Z., *Tribology*, McGraw-Hill, 1979, pp. 273–274.

16 Hashimoto, H., and Wada, S., "An Influence of Inertia Forces on Stability of Turbulent Journal Bearings," *Bulletin of JSME*, Vol. 25, 1982, pp. 653–662.

17 Hashimoto, H., and Wada, S., "An Analysis of Dynamic Characteristics of Turbulent Journal Bearings Considering Inertia Forces," *Bulletin of JSME*, Vol. 25, 1982, pp. 1601–1609.

18 Hashimoto, H., Wada, S., and Ito, J., "An Application of Short Bearing Theory to Dynamic Characteristic Problems of Turbulent Journal Bearings," ASME Journal of Tribology, Vol. 109, 1987, pp. 307–314.

Downloaded 16 Aug 2012 to 165.91.101.108. Redistribution subject to ASME license or copyright; see http://www.asme.org/terms/Terms_Use.cfm